Journal of Applied Polymer Science

Fabrication and Properties of Nano Indium Tin Oxide/Wool Keratin Composites

Rong Li,[1,2] Jinsong He,[1,2] Feng Wen,[1,2] Dong Wang[2]

[1]Key Laboratory of Science and Technology of Eco-Textiles (Ministry of Education), Donghua University, People's Republic of China
[2]National Engineering Research Center for Dyeing and Finishing of Textiles, Donghua University, People's Republic of China
Correspondence to: R. Li (E-mail: lirong@dhu.edu.cn)

ABSTRACT: A functional keratin/indium tin oxide (ITO) composite was prepared by a route involving an ionic liquid dissolving process and a wet-chemical codeposition technique. The crystal structure and morphology of ITO were investigated by X-ray diffraction and transmission electron microscopy, respectively. The factors influencing the crystal structure and the size of the ITO were investigated in detail. The optimal In/Sn ratio, reaction temperature, and pH value were found to be 10:1, 70°C, and 7, respectively. The sheet resistance of the composite reached 0.39 kΩ/□. In addition, the composite films possessed a perfect UV protection ability with a UV protection factor of up to 43.78. © 2013 Wiley Periodicals, Inc. J. Appl. Polym. Sci. **2014**, *131*, 39641.

KEYWORDS: biopolymers & renewable polymers; ionic liquids; membranes; nanoparticles; nanowires and nanocrystals

Received 30 November 2012; accepted 9 June 2013
DOI: 10.1002/app.39641

INTRODUCTION

Wool keratin fiber, one of the earliest natural fibers used by human beings, is considered an important raw material in the textile industry because of its excellent mechanical and thermal properties. A great quantity of short fibers and crude fibers are discarded during wool weaving every year, and a mass of waste wool keratin textile fibers are abandoned in our daily life; this not only causes a waste of keratin resources but also pollutes the environment.[1] Because about 50 wt % of these waste wool fibers are made of keratin, a usable protein, they have been regarded a renewable resource worthy of a better study of the recycling of waste wool fibers for effective utilization. Keratin molecules, which are not dissolved under normal conditions, are highly crosslinked, three-dimensional stable structures with disulfide bonds, hydrogen bonds, salt bonds, and other bonds.[2] Therefore, the dissolution procedure of keratin is the basis and premise of using these renewable resources. The key step of the preparation of a keratin solution is to make the bonds rupture; this provides crosslink between the keratin macromolecules. At present, there are several methods for obtaining wool keratin solutions, such as the oxidation method, the reduction method, and ionic liquids. Yu and Fan[3] reported that anisotropic cortical cells could be extracted from waste wool fibers by formic acid ultrasonic treatment and could be successively included in different proportions in a chitosan matrix to make film-forming composites suitable for film casting and filament spinning. Among all of the methods listed previously, ionic liquids, which can also be called *room temperature molten salts* and are typically composed of organic cations and large anions,[4] are quite unique for their low volatility, wide liquid range, good thermal stability, strong solvent power for organic and inorganic compounds, high ionic conductivity, and wide electrochemical window.[5] Because of these special structures compared to the traditional molecular solvents, ionic liquids as solvents for the dissolution of natural polymer materials (e.g., cellulose and silk protein) and the preparation of nanoparticles, have exhibited promising applications in materials science.[6–8] Researchers have used 1-allyl-3-methylimidazolium chloride ($[AMIM]^+Cl^-$) and 1-Butyl-3-methylimidazolium Chloride $[BMIM]^+Cl^-$ as solvents to dissolve wool fabric and have measured the properties of regenerated films.[9]

Indium tin oxide (ITO) is receiving a great deal of attention because of its outstanding optical and electrical properties. ITO is the most widely used transparent conducting oxide material for its excellent characteristics in conductivity and optical transparency and its good surface features.[10,11] Thus, it has a wide variety of applications, including flat panel displays, functional glass, and solar cells.[12] Several synthesis and processing methods for making ITO nanostructures have been reported. One of the approaches is based on thin-film deposition; another uses solution-based synthesis. ITO can be fabricated in the form of thin films with various techniques, such as physical and chemical vapor deposition, which are quite cost intensive.[13] Solution-based approaches, including solvothermal synthesis and the

coprecipitation method, have gained more popularity over the deposition approach. Kanga et al.[14] reported that ITO nanospheres of various sizes can be synthesized by the selective etching of ITO thin films with diluted HCl solution as the etchant. Moreover, the sizes of the ITO nanospheres can be readily controlled by variation of the thicknesses of the ITO films. Ding et al.[15] synthesized nanoscale ITO particles with a distribution of particle size of 30–90 nm by liquid-phase coprecipitation method under given conditions with solutions of indium chloride, tin chloride, ammonia, and two kinds of surfactants as dispersants. In the consideration of a fast and inexpensive fabrication method, the wet-chemical deposition of ITO nanoparticles as an alternating approach should be preferred.

Although many successes have been focused on the optoelectrical properties of ITO fabricated on glass or on plastic foil, little work has been done to discuss the properties of its composite films prepared on other substrates. In this study, a functional composite of wool keratin and nano-ITO was successfully prepared by a new and simple method. The process involved the following steps: (1) dissolving the wool keratin fibers with a new type of green solvent, ionic liquids; (2) adding the ITO powder prepared by the coprecipitation method into wool/ionic liquid solution, and finally (3) obtaining the composite material by its regeneration from a wool/ionic liquid solution. The structures and optoelectrical properties of the functional composite were also studied.

EXPERIMENTAL

Materials and Chemicals

The wool keratin fibers samples were provided by Ningbo Reward Wool Industry Co., Ltd. Ionic liquids (99% $[AMIM]^+Cl^-$) were supplied by Shanghai Cheng Jie Chemical Co., Ltd. Detergent 209 (*N,N*-sodium oleoyl methyl taurinate) was obtained from Shanghai Jing Wei Chemical Co., Ltd. Other chemicals, including acetone (analytical reagent), anhydrous ethanol (analytical reagent), indium (high-purity), tin tetrachloride pentahydrate (analytical reagent), hydrochloric acid (analytical reagent), and ammonia (analytical reagent), were used as received without further purification and were purchased from Sinopharm Chemical Reagent Co., Ltd. Deionized (DI) water was used throughout the course of this investigation.

Dissolution of Wool Keratin Fibers

The wool keratin fibers were used in the following procedures before solubility experiments. They were first washed by detergent 209 and then cleaned by 200 mL of a mixture of acetone and ethanol (molar ratio 1:1) in a Soxhlet extractor for 12 h. Finally, we rinsed them with DI water and dried them at 100°C for 12 h in an oven. An amount of 10.0 g of $[AMIM]^+Cl^-$ was placed in a 50-mL, three-necked flask and heated to 130°C to obtain a homogeneous solution, and we then began stirring. After that, the pretreated wool keratin fibers were cut into short lengths (5 mm), and we added 0.1 g of keratin fibers to the ionic liquid solution every time until the added wool keratin fibers completely dissolved.

Preparation of ITO Powders

A certain amount of indium was dissolved in a hydrochloric acid solution, and the mixture was stirred at 80°C. After dissolution, an $InCl_3$ solution was obtained by dilution with DI water. $SnCl_4$ solution (In/Sn = 8:1, 9:1, 10:1, 11:1, and 12:1) and ammonia (20%) were dropped into $InCl_3$ solution at a rate of 10 drop/min under vigorous stirring. The pH value of the reaction solution was adjusted to 5–9 by ammonia. After that, the mixture was kept stirring for 30 min at different temperatures (50, 70, and 90°C) and then maintained for aging for 2 h at room temperature. Subsequently, the precipitates were observed and washed with DI water (4–5 times) and ethanol (twice); this was followed by vacuum freeze drying for 24 h. Finally, the powder specimens placed in a furnace, and the temperature was increased to 400, 500, and 600°C at a rate of 3°C/min and maintained at these different temperatures for 2 h each. All of the experiments were done once.

Synthesis of Wool Keratin and ITO Composites

The as-prepared ITO powders were added to the ionic liquid/wool keratin solution to achieve an ITO/solution ratio of 1 wt %. The solution became homogeneous after vigorous stirring at 100°C for 30 min and treatment in an ultrasonic bath for 20 min. Glass slides were used as substrates, and they were cleaned with acetone, ethanol, and DI water in ultrasonic bath for 5 min, respectively, before use. The mixture solution was spread evenly on the glass at a thickness of 0.3–0.5 cm. The glass slide was immersed in DI water for 6 h at room temperature in a sealed dish and stored for another 6 h after the water was renewed. After that, an opalescent composite film was obtained by several washings with DI water and drying at 50°C. The composite film was taken from the glass slide and stored for characterization. The ionic liquid could be recycled by the removal of the solvent from the solution of ionic liquid mixed with water with a rotary evaporator (Eyela N-1000).

Characterization

The crystal structures of the as-prepared ITO powders were analyzed by X-ray diffraction (XRD) spectra (Rigaku D/max-2550, Cu Kα line = 1.54 Å, operating at 40 kV and 200 mA, scanning speed = 0.02°/min). The morphologies of the composites were observed by a transmission electron microscope (JEOL JEM-2100F, operating at 200 kV). The surface electrical resistance of the composite film was measured by a four-probe method by a SZT-2A four-probe tester (Tongchuang Technology Co., Suzhou, China). The UV-screen properties of the composite film were investigated according to AATCC 183–2000 by a UV transmission spectrometer (Labsphere UV-1000F, wavelength range = 250–400 nm).

RESULTS AND DISCUSSION

Solubility of the Wool Protein Fibers in the Ionic Liquids

The dissolution process is briefly described here, and a detailed discussion can be found in our previous work.[9] The wool keratin fibers underwent the following procedures before the solubility experiments: first, we washed them with Detergent 209, then cleaned them with 200 mL of a mixture of acetone and ethanol (molar ratio = 1:1) in a Soxhlet extractor for 12 h, and finally rinsed them with DI water and dried them at 100°C for 12 h in an oven. $[AMIM]^+Cl^-$ (10.0 g) was placed in a 50-mL, three-necked flask and heated to 130°C to obtain a homogeneous solution, and we then began to stir the mixture. After that,

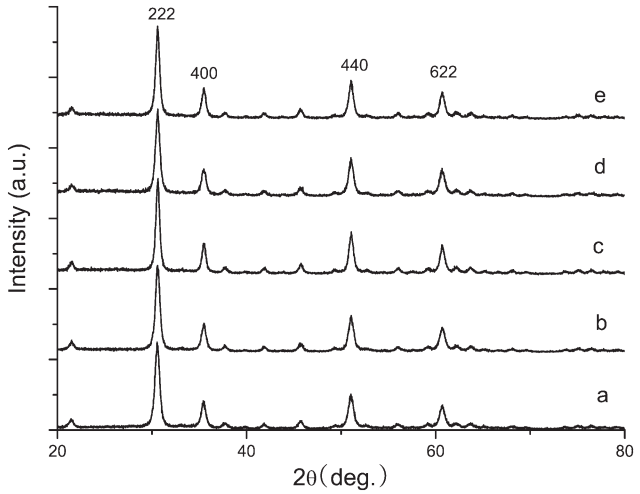

Figure 1. XRD patterns of the ITO samples with different In/Sn molar ratios: (a) 8:1, (b) 9:1, (c) 10:1, (d) 11:1, and (e) 12:1.

the pretreated wool keratin fibers were cut into short lengths (5 mm), and we added 0.1 g of keratin fibers to the ionic liquid solution every time until the added wool keratin fibers completely dissolved. Different dissolution times (1, 3, 5, 10, and 15 min) were set for the dissolution procedure of the wool keratin fibers in $[AMIM]^+Cl^-$. At first, the wool protein fibers swelled in the ionic liquids. As the fibers continued dissolving, the keratin fibers gradually became thinner and finally disappeared. In the swelling stage, ionic liquids as solvents penetrated into the molecule intervals of the wool keratin from the outer layers to the inner ones. The intervals of molecules increased, and the volumes of the keratin fibers swelled as a salvation effect proceeded; this gradually reduced the interactions between the molecules. In the dissolution stage, the chains were untangled because of complete salvation, moved from a high concentration to a lower concentration, and finally dissolved.

Effect of the ITO In/Sn Ratio

Different In/Sn ratios (8:1, 9:1, 10:1, 11:1, and 12:1) were set for the reaction temperature of 70°C and the pH of 7. Figure 1 shows the XRD patterns of ITO obtained by the coprecipitation process with different In/Sn ratios. All diffraction peaks of the XRD patterns could be indexed as the pure bixbyite phase of In_2O_3 (joint committee on powder diffraction standards (JCPDS) card number 6–0416) and no characteristic peaks of Sn or its compounds were observed, even when the amount of doped Sn was increased. This result reveals that the doping of Sn into In_2O_3 resulted in neither an XRD pattern shift nor an additional pattern of SnO_2; this implied that Sn ions may have been distributed into the In_2O_3 lattices rather than forming a new phase.[16] The maximum peak intensity is shown in Figure 1(c) and indicates that a better crystalline perfection was achieved at a molar ratio of In/Sn = 10:1.

Effect of the Reaction Temperature

Figure 2 shows the transmission electron microscopy (TEM) images of the ITO powders, which were prepared under the same In/Sn molar ratio of 10:1 and at a pH value of 7 but at different reaction temperatures (50, 70, and 90°C) The supersaturation of the solution being related to the temperature had a direct impact on the nucleation and growth of the crystals. In general, the growth rate of the crystal nucleus increased with

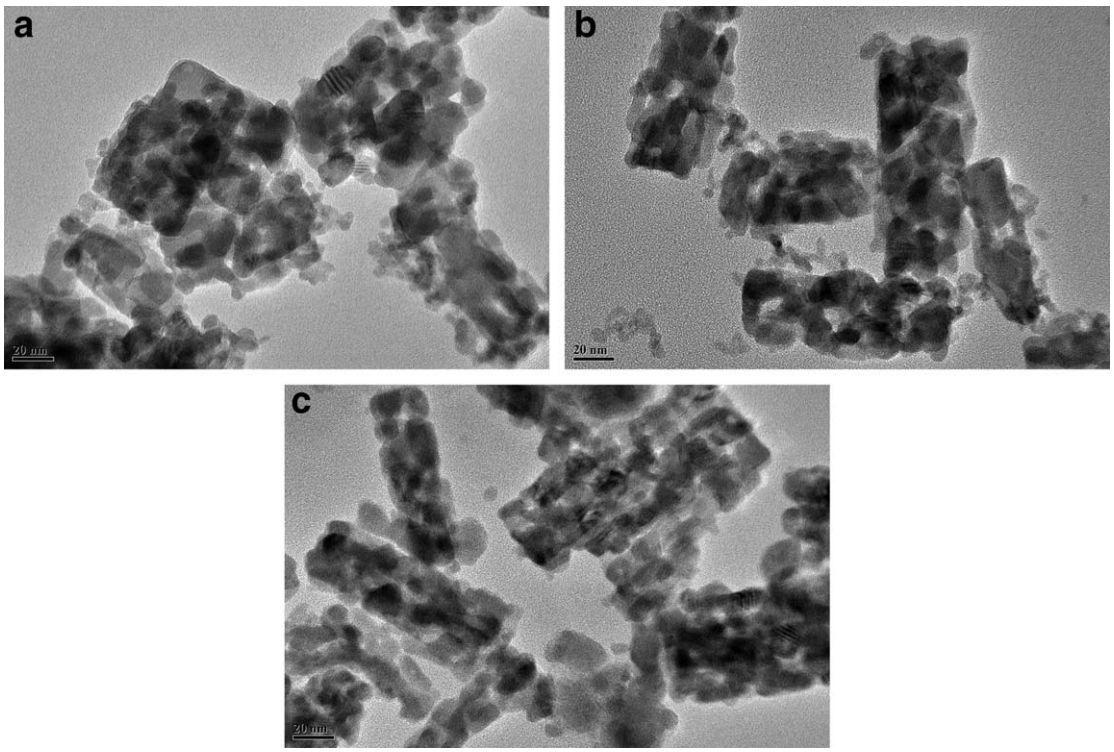

Figure 2. TEM images of the ITO nanoparticles at different reaction temperatures: (a) 50, (b) 70, and (c) 90°C.

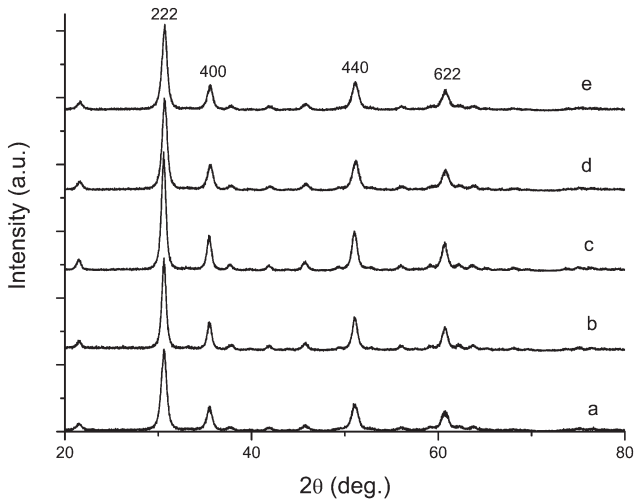

Figure 3. XRD patterns of the ITO nanoparticles prepared at various pHs: (a) 5, (b) 6, (c) 7, (d) 8, and (e) 9.

increasing degree of supersaturation and decreased with increasing viscosity of the dispersion medium. On the other hand, reducing the temperature increased both the viscosity of the medium, which controlled the diffusion rate, and the supersaturation degree. Therefore, a high growth rate of crystal nucleus was achieved at a certain temperature. It was clear that the mean size of the ITO nanoparticles increased with increasing reaction temperature. At a lower temperature of 50°C, a more supersaturated reaction solution was propitious to the nucleation of the ITO crystallites, whereas this behavior was unfavorable to the growth of the crystal nucleus. Thus, a small particle size of ITO was obtained at around 20 nm, as shown in Figure 2(a). Moreover, the Brownian movement was decelerated at lower reaction temperatures, and this also restricted the growth rate of the ITO crystals because of lower chance of ionic or molecular collision.[17] Figure 2(b) shows that a higher temperature of 70°C favored the growth of the crystalline nucleates, and the ITO nanoparticles exhibited a rodlike structure with a size 20–30 nm in diameter, and 60–100nm in length. As shown in Figure 2(c), the ITO particles tended to aggregate severely because of their faster growth rate when the temperature was up to 90°C. On the basis of the previous analytical results, a reaction temperature of 70°C was selected for the experiments; this temperature favored both nucleation and the growth of the crystal nucleus.

Effect of the pH Value

Different pH values ranging from 5 to 9 were used to prepare ITO powders while he In/Sn ratio was kept at 10 and the temperature was kept at 70°C. Figure 3 compares the diffraction patterns for the as-prepared samples. All of the peaks corresponded to the diffraction data for bixbyite indium oxide as well, and there were no measurable amounts of other crystalline species; this indicated that the pH had little effect on the crystalline structure of the ITO powders. The only difference among the XRD patterns was the intensity of the diffraction peak. In comparison with the other samples, the resulting ITO particles at pH 7 presented a higher crystallinity, as indicated by a stronger diffraction peak. The pH value was a key factor in controlling the degree of supersaturation. With increasing pH from 5 to 7, the ITO crystallites grew with the increasing concentration of hydroxide precursors. The growth process was controlled by diffusion. Further increases in the pH value led to an instantaneous nucleation and made the hydroxide concentration decrease sharply; this influenced the crystalline perfection accordingly.

Effect of Calcination

Figure 4 shows the XRD patterns of the ITO precursors and ITO powders calcined at different temperatures (400, 500, and 600°C) for 2 h. In the XRD pattern of the noncalcined ITO, the diffraction peaks were identical to the available data of $In(OH)_3$ (JCPDS card number 16–0161). However, some amorphous domains could also be observed; these may have been due to the existence of a small amount of $Sn_3O_2(OH)_2$ (JCPDS card number 25–1303). The large space among the grains of indium hydroxide facilitated doping. This was why Sn^{4+} could be finely doped into In_2O_3. For the calcined ITO powders, different XRD patterns were observed; these were well consistent with the pure bixbyite phase of In_2O_3 without the formation of a secondary phase and clusters. The intensities of the diffraction peaks improved with increasing calcined temperature, and the crystallinities determined from the full-width at half-maximum values showed the same trend. It should be noted that in ITO, there was a phase transition though the calcined procedure. The TEM results, as shown in Figure 5, also confirmed that calcined ITO powders had a better crystalline perfection and larger particle size that the noncalcined ITO precursors. This implied further that thermal treatment was favorable for the complete transformation of $In(OH)_3$ crystallites into In_2O_3 crystallites. High-resolution TEM images showed nanometer-scale In_2O_3/Sn with a spherical to cubic morphology [Figure 5(c)]. Highly ordered lattice fringes, even in the surface region, were evidence of the crystallinity of the particles.

Electrical Properties of the Wool Keratin and ITO Composites

The effect of the In/Sn ratio on sheet resistance is shown in Figure 6. ITO nanoparticles were prepared under an In/Sn molar

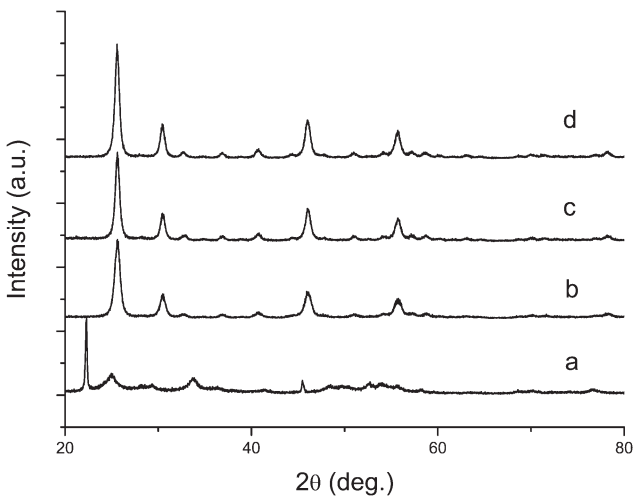

Figure 4. XRD patterns of the ITO samples: (a) without thermal treatment, (b) calcined at 400°C for 2 h, (c) calcined at 500°C for 2 h, and (d) calcined at 600°C for 2 h.

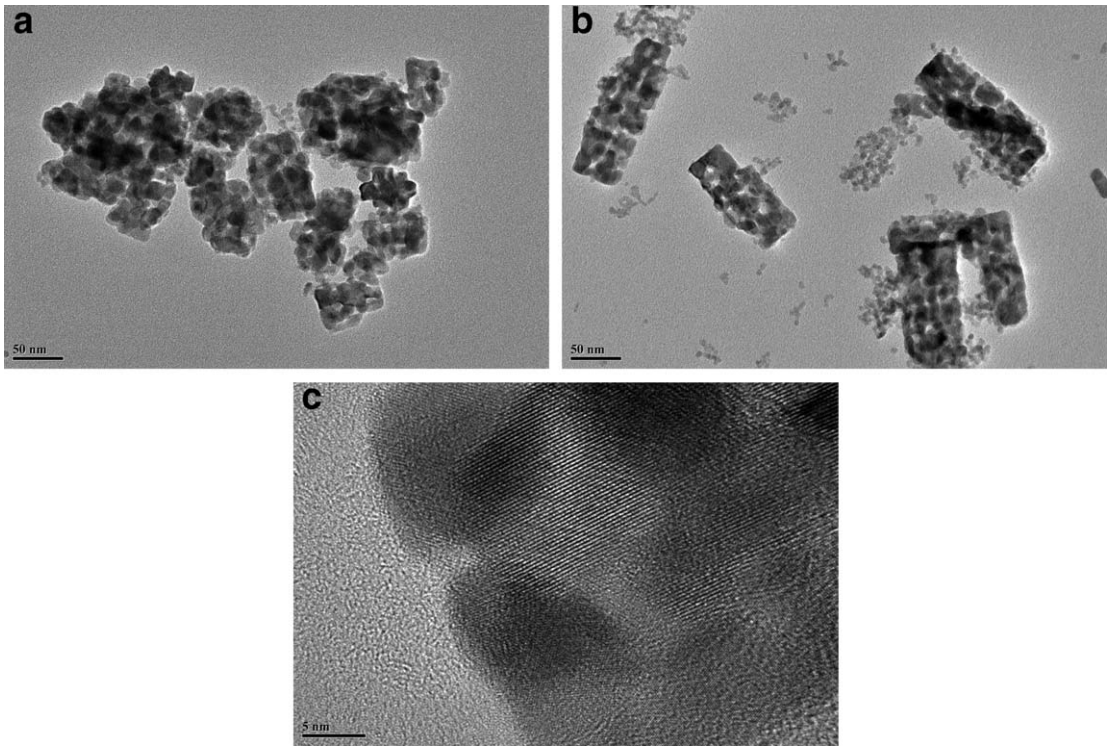

Figure 5. TEM images of the ITO samples: (a) without thermal treatment and (b) calcined at 600°C for 2 h. (c) High-resolution TEM image of panel b showing lattice fringes.

ratio of 10:1, a pH value of 7, and a reaction temperature at 70°C and were then calcined at 600°C for 2 h. It is worth noting that the sheet resistance decreased with increasing amount of Sn when the In/Sn ratio was less than 10:1 and then increased at a higher In/Sn ratio; this suggested that the amount of doped Sn was a key factor in controlling the conductivity of the composite film. This phenomenon was due to the incomplete formation of the oxygen vacancies at lower contents of Sn; this led to a lower conductivity of the composite film. However, the sheet resistance increased adversely when the doping amount was further decreased, that is, at an In/Sn ratio of 11 or 12. This effect was assumed to be the lattice contraction and the decrease of lattice constant induced by a higher doping amount, which resulted in a strong scattering of the electrons and a decrease in the carrier mobility. Thus, a minimum sheet resistance of 0.39 kΩ/□ was obtained with an In/Sn ratio of 10; this was consistent with the XRD results. In comparison, commercially available magnetron-sputtered ITO coatings exhibited a sheet resistance of 10–20 Ω/□.[18] This massive difference in the conductivity occurred mainly without the establishment of a

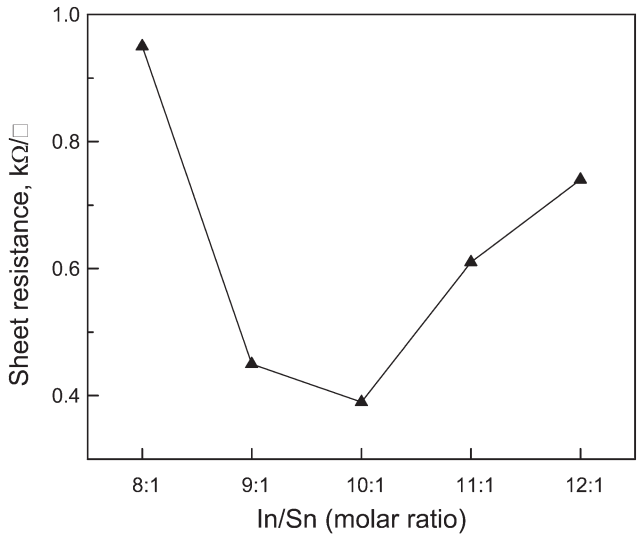

Figure 6. Sheet resistance of the keratin and ITO composite films with different In/Sn ratios (8:1, 9:1, 10:1, 11:1, and 12:1).

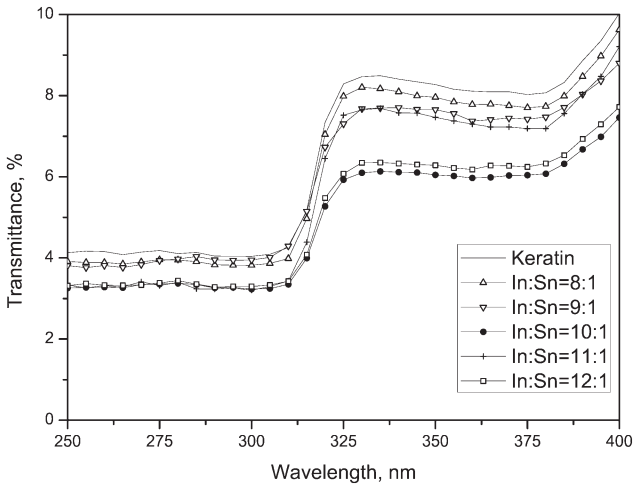

Figure 7. UV transmittance of the keratin/ITO composite films with different In/Sn ratios.

Table I. UPFs for the Keratin/ITO Composite Films with Different In/Sn Ratios

		In/Sn molar ratio				
Sample	Keratin	8:1	9:1	10:1	11:1	12:1
UPF	20.42	34.19	38.50	43.78	42.65	40.12

sufficient carrier concentration (1 wt % ITO) and without a homogeneous distribution in this study.

UV-Screen Properties of the Wool Keratin/ITO Composite Films

Figure 7 presents the UV transmittance of the composite films prepared with different In/Sn ratios. The obvious UV absorption appeared at wavelengths ranging from 250 to 400 nm; this indicated effective UV absorption properties for composites. As shown in Figure 7, the UVB transmittance (295–315 nm) was not found to be significantly associated with the difference in the content of doped Sn. Otherwise, it was clear that the UVA transmittance (315–400 nm) decreased with increasing content of doped Sn and then increased at an In/Sn ratio higher than 10. The values of the UV protection factor (UPF) listed in Table I show the same changing trends. Another interesting phenomenon was that the maximum UPF of 43.78 was also achieved at an In/Sn ratio of 10; this implied that the UV absorbency was related to the crystal structure of ITO. Thus, the as-prepared composites could effectively protect against UV radiation. As a result, it could potentially be applied to UV-shielding materials, such as fibers, coatings, cosmetics, and plastics.[19]

CONCLUSIONS

In summary, a functional keratin/ITO composite film was synthesized via an inexpensive and reproducible method. It was demonstrated that wool keratin could be dissolved in ionic liquids effectively. The effect of the doped Sn, temperature, and pH on the crystallinity and morphology of the ITO particles was investigated in detail. The XRD and TEM analysis revealed the crystal structure of the as-prepared ITO powders had a bixbyite crystal structure with a high crystallinity, and the size of the ITO rods was estimated to be 20–30 nm in diameter, and 60–100nm in length. The optimal performances of ITO were obtained at a molar ratio of In/Sn = 10, a reaction temperature of 70°C, and a pH of 7 in this study. The composites presented good electrical and UV-shielding properties, and these are suggested to have been related to the crystallinity of the composites. These results indicate that the composites have potentially remarkable applications of interest.

REFERENCES

1. Lv, L. H.; Yu, Y. L.; Zhou, J. *Tekstil* **2010**, *59*, 201.
2. Hames, B. D.; Hooper, N. M. Biochemistry; Science Press: Beijing, **2003**.
3. Fan, J.; Yu, W. *Waste Manage. Res.* **2010**, *28*, 44.
4. Ding, K.; Miao, Z.; Hu, B.; An, G.; Sun, Z.; Han, B.; Liu, Z. *Langmuir* **2009**, *26*, 5129.
5. Miao, S.; Liu, Z.; Miao, Z.; Han, B.; Ding, K.; An, G.; Xie, Y. *Micropor. Mesopor. Mater.* **2009**, *117*, 386.
6. Bühler, G.; Zharkouskaya, A.; Feldmann, C. *Solid State Sci.* **2008**, *10*, 461.
7. Miao, S.; Miao, Z.; Liu, Z.; Han, B.; Zhang, H.; Zhang, J. *Micrpor. Mesopor. Mater.* **2006**, *95*, 26.
8. Bühler, G.; Thölmann, D.; Feldmann, C. *Adv. Mater.* **2007**, *19*, 2224.
9. Li, R.; Wang, D. *J. Appl. Polym. Sci* **2013**, *127*, 2648.
10. Lewis, B. G.; Paine, D. C. *MRS Bull.* **2000**, *25*, 22.
11. Li, Z. Q.; Lin, J. J. *J. Appl. Phys.* **2004**, *96*, 5918.
12. Gilstrap, R. A., Jr.; Summers, C. *J. Thin Solid Films* **2009**, *518*, 1136.
13. Ray, S.; Banerjee, R.; Basu, N.; Batabyal, A. K.; Barua, A. K. *J. Appl. Phys.* **1983**, *54*, 3497.
14. Kanga, J. H.; Uthirakumarb, P.; Katharriaa, Y. S.; Ryua, J. H.; Kima, H. K.; Kima, H. Y.; Hana, N.; Parka, Y. J.; Beaka, Y. S.; Kima, S. M.; Honga, C. H. *Appl. Surf. Sci.* **2012**, *258*, 8996.
15. Ding, Z.; An, C.; Li, Q.; Hou, Z.; Wang, J.; Qi, H.; Qi, F. *J. Nanomater.* **2010**, Article ID 543601, 5 pages, doi:10.1155/2010/543601.
16. Sun, Z.; He, J.; Kumbhar, A.; Fang, J. *Langmuir* **2010**, *26*, 4246.
17. Chen, Z.; Li, X. X.; Du, G.; Chen, N.; Suen, A. Y. M. *J. Lumin.* **2011**, *131*, 2072.
18. Heusing, S.; de Oliveira, P. W.; Kraker, E.; Haase, A.; Palfinger, C.; Veith, M. *Thin Solid Films* **2009**, *518*, 1164.
19. Tang, E.; Cheng, G.; Pang, X.; Ma, X.; Xing, F. *Colloid Polym. Sci.* **2006**, *284*, 422.